# Preparation of Co-Doped Graphitic Carbon Nitride and Degradation of MB by Heterogeneous Photo-Fenton-like Reaction System

**DE-LI NIU, KAI BAO, XUAN-YE HUANG, MAO-JUAN BAI\*, JUN WAN\***

College of Environment and Safety Engineering, Qingdao University of Science and Technology, Qingdao 266042, China

*Abstract: In this study, Co-porous-g-C₃N₄(porous Co-Doped graphitic carbon nitride) was synthesized by a one-step calcination method successfully. Co-porous-g-C₃N₄ was characterized by transmission electron microscopy, X-ray photoelectron spectroscopy, UV-vis diffuse reflectance, and specific surface area determination. The Photo- Fenton-like system was successfully constructed under the condition of coexistence of Co-porous-g-C₃N₄ and H₂O₂. The synergistic effect of Fenton-like system and photo-catalysis was realized. Through the optimization of experimental conditions, the best photocatalytic performance of this heterogeneous reaction system was achieved. The degradation rate of MB (methylene blue, 40 mg/L) could reach 98.3% at 90 min. Co-porous-g-C₃N₄ had photocatalytic degradation activity for different organic pollutants and had wonderful recyclability and stability. The main degradation effect was attributed to ·O₂- which could be generated through two channels in the Photo- Fenton-like system. Moreover, the rate of photogenerated electron-hole complexation could be decreased due to the reaction of low-valent cobalt and photoelectrons in this heterogeneous reaction system.*

*Keywords: Co-Doped graphitic carbon nitride, MB, Photo-Fenton-like reaction, photocatalysis*

## 1.Introduction

Photocatalytic technology, an excellent oxidation technology, was widely used in disposing organic pollutants [1], and typical photocatalysts are normally divided into metal oxide [2-4], selenide and sulfide [5-7], and non-metallic semiconductor [8-9]. However, there are still some limits in practical application, due to the inherent properties of semiconductor. Notably, photocatalytic technology has good cooperativity with other advanced oxidation technologies, for example Fenton oxidation technology [10]. In a nutshell, Photo-Fenton reaction system would be constructed by visible-light, hydrogen peroxide and photocatalysts that was modified by transition metal, such as Fe, Co, Cu.

Graphitic carbon nitride (g-C₃N₄), a green and excellent photocatalyst, possesses many advantages such as visible light response, environmental friendliness, suitable band gap (2.7 eV) and stability [11]. It is widely used in many fields as organic pollutants treatment [12], H₂ evolution [13], harmful gas treatment [14], supercapacitors [15], N₂ fixation [16] and so on. However, g-C₃N₄ has some defects that can limit the application. But these defects can be improved by various modification methods, such as metal and non-metal doping [17-18], Z-scheme and S-scheme heterojunction [19-20], polymerizing g-C₃N₄ with other semiconductors [21-22] and precursor pretreatment [23]. It is worth noting that the ionic radius of transition metals and g-C₃N₄ are similar, so the transition metal doping is beneficial to g-C₃N₄ to form more active sites and improve the photocatalytic ability. Therefore, the transition metal doping is one of the best modification methods.

Transition metal (cobalt) doping was used in various semiconductor composites. The physical and chemical properties of cobalt element are similar to iron and nickel elements. Wook Ahn et al. [24] designed a ternary transition (Ni, Co, Fe) metal-doped porous organic framework electrocatalyst (NCF-MOF). The novel NCF-MOF electrocatalyst exhibited a well-coordinated electronic structure, which has a larger active specific surface area and more mass transfer pathways.

*\* email: wanjundz@sohu.com, 734266042@qq.com*

Jianping Ai et al. [25] synthesized Co-ZnO powder by hydrothermal method and Co doping which possessed high crystallinity and magnetism at room temperature. The photocatalytic efficiency of Co-ZnO was studied, the methyl orange degradation reached 89.8% at 3 h.

At the meantime, graphitic carbon nitride also can be modified by cobalt element. Co-doping can not only retain the advantages of g-$C_3N_4$, but also can make up for the defects of g-$C_3N_4$. Yalin Yu et al. [26] prepared cobalt-oxygen co-doped graphite carbon nitride (Co-$OCN_{VN}$) by thermal polymerization method. The conclusion showed that the cobalt element existed in the form of cobalt-nitrogen bond ($Co^{2+}$-$N_x$), instead of cobalt oxygen compound ($Co_xO_y$). The photocatalytic had a higher activity for the degradation of Bisphenol A (BPA). Also, D. Das et al. [27] synthesized a cobalt-doped graphite carbon nitride (CoGCN) photocatalyst through a thermal polymerization process. Although, the structure of g-$C_3N_4$ was not changed due to the doping of cobalt, the results proved that the specific surface area of CoGCN and the degradation of Eosinbluish increased. However, the layered structure of g-$C_3N_4$ has not been changed by simple cobalt-doping, which led to little promotion of photocatalytic ability. In addition, the precursor modification is also a advantageous way to optimize the photocatalytic ability of g-$C_3N_4$.

Herein, we intend to prepare Co-g-$C_3N_4$ by hydrochloric acid (37%) and cobalt chloride, which possess poriferous microstructure and excellent photocatalytic ability. Under the combined action of Co-g-$C_3N_4$, visible light and hydrogen peroxide (30%), the Fenton-like system was established. And the degradation effect of methylene blue was investigated in different conditions. As a consequence, cobal-doping with the auxiliary of hydrochloric acid (%) is an effective pathway to dispose organic pollutants.

## 2 Materials and methods

### 2.1 Materials

Melamine ($C_3N_3(NH_2)_3$), cobalt chloride ($CoCl_2 \cdot 6H_2O$), 37% hydrochloric acid (37% HCl), methylene blue (MB), 30% hydrogen peroxide (30% $H_2O_2$), ethylenediaminetetraacetic acid disodium salt (EDTA-2Na), tert-butanol (TBA), benzoquinone (BQ), ethanol ($C_2H_5OH$) were bought from Sinopharm Chemical Reagent Co., Ltd.

### 2.2. Preparation of porous Co-g-$C_3N_4$ photocatalyst

The poriferous Co-g-$C_3N_4$ was synthesized as follows: 2.5g melamine was dispersed in hot deionized water under magnetic stirring, and then 37% hydrochloric acid was dropped into the solution which contained melamine slowly. The mixture solution naturally cooled at room temperature. An appropriate amount of cobalt chloride was added into the mixture under magnetic stirring and maintained 30 min to keep homogeneous, the precursor solution was prepared. Subsequently, the precursor solution was dried and then put into a crucible with cover. This crucible was annealed at 500℃ for 2 h and 520℃ for 2 h in air atmosphere with the heating rate of 5℃·$min^{-1}$. After cooling to room temperature, the photocatalysts were prepared. The photocatalyst treated with hydrochloric acid was recorded as Co-porous-g-$C_3N_4$, and the photocatalyst not treated with hydrochloric acid was recorded as Co-g-$C_3N_4$.

### 2.3. Photocatalytic exploration Experiment of Co-porous-g-$C_3N_4$

Photocatalytic optimization analyses were carried out on a photocatalytic reactor, equipped with a steel shell, a magnetic stirrer, a condenser equipment and a 500 W xenon lamp. A certain amount of as-prepared Co-porous-g-$C_3N_4$ was added into the cylindrical quartz tube that included 50 mL methylene blue reaction solution under magnetic stirring. After stirring in dark for 40 min, the reaction system switched on the xenon lamp to simulate visible light, and then added 30 % $H_2O_2$. During the process of continuous irradiation, 5 mL of the reaction mixture that was filtered by 0.45 µm water-based membrane system was drew at a given illuminated time intervals and then the concentration of MB was monitored by a UV-vis spectrophotometer at 664 nm. The degradation effect of Co-porous-g-$C_3N_4$ would be reflected in the concentration ratio of MB in different time.

## 3. Results and discussions

### 3.1. Characterization of Co-porous-g-C₃N₄

In order to analyse the internal composition of as-synthesized Co-porous-g-$C_3N_4$, the photocatalyst had been characterized by several ways, such as X-ray diffraction, UV-Vis DRS spectra, X-ray photoelectron spectroscopy, transmission electron microscope and so on. XRD (D/MAX-2500/PC) patterns of g-$C_3N_4$ and Co-porous-g-$C_3N_4$ were revealed in Figure 1, which 2θ ranged from 10° to 70°. There are two distinct peaks at 12.9° and 27.4°. These two peaks are related to the (100) inter-planar stacking and (002) inter-planar stacking of g-$C_3N_4$. Compared to g-$C_3N_4$ and Co-porous-g-$C_3N_4$, the positions of characteristic peak were basically the same, but the peak intensity of Co-porous-g-$C_3N_4$ was stronger due to the high crystalline degree of polymer. This may be due to the addition of hot water and hydrochloric acid during the melamine treatment, which will partially hydrolyze melamine into cyanuric acid. The presence of cyanuric acid is more conducive to the polymerization of g-$C_3N_4$.
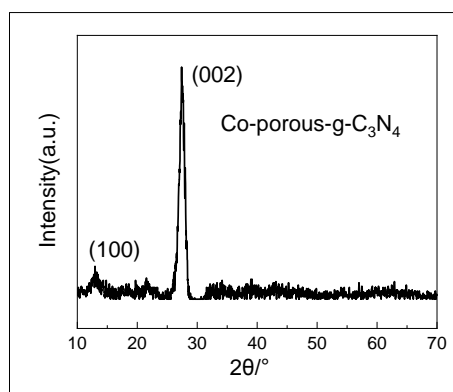


**Figure 1.** XRD pattern of Co-porous-g-C₃N₄

The morphology of g-$C_3N_4$ and Co-porous-g-$C_3N_4$ were characterized by SEM (JSM-6700F) analysis, and the micro-structures were characterized by TEM (JEM-F200) analysis. The results were showed in Figure 2. The SEM (Figure 2a-b) and TEM (Figure 2c-d) images of Co-g-$C_3N_4$ reveal distinct porous structure that distribute regularly at the whole photocatalyst, indicating that the Co-porous-g-$C_3N_4$ photocatalyst possesses larger surface area and more active sites compared with g-$C_3N_4$ which was prepared in previous study [28]. Moreover, there are no distinct black particles of metals or metal compounds that was observed by the images of Co-porous-g-$C_3N_4$, the result Corresponding to the analysis of XRD.
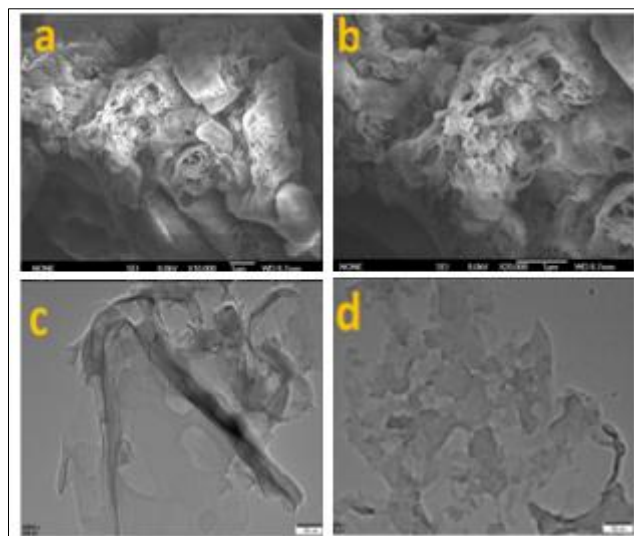


**Figure 2.** SEM (a, b) and TEM (c, d) images of Co-porous-g-C₃N₄

The corresponding element composition of Co-porous-g-C₃N₄ was characterized by EDS (JSM-6700F) analysis. As showed in Table 1, the C, N, O and Co atoms were observed, the C and N originated from g-C₃N₄ and then the Co originated from cobalt chloride added during the photocatalyst preparation process. Besides, Co element content is 0.61wt%. The result indicated that the cobalt-doped porous g-C₃N₄ photocatalyst was successfully synthesized.

**Table 1.** EDS data of Co-porous-g-C₃N₄

| Element | C | N | O | Co |
|---------|-----|-----|-----|-----|
| Weight% | 30.48 | 60.39 | 7.53 | 0.61 |

For ascertaining the chemical states and the connection states of element, XPS (JSM-6700F) spectra of Co-porous-g-C₃N₄ was studied in Figure 3. As showed in Figure 3, the existence of C 1s, N 1s and Co 2p have been researched in detail. There are two distinct peaks of C 1s located at 285.3 and 288.5 eV in Figure 3a, which ascribe to $sp^2$-hybridized C-C and triazine ring N-C=N, respectively. In Figure 3b, three peaks of N 1s spectrum were studied, that located at 398.2, 399.5 and 400.6 eV, their energies correspond to $sp^2$-hybridized nitrogen (N-C=N), $sp^3$-tertiary nitrogen (N-(C)₃) and CH-N bond, respectively. It is also obvious that three constituent peaks of Co 2p were shown in Figure 3c, two peaks of which located at 781.8 and 796.7 eV, associating with Co $2p_{3/2}$ and Co $2p_{3/2}$, respectively. The other peak located at 785.4 eV which ascribed to the satellite peak of Co element. These peaks of Co 2p did not match metallic Co, Co oxide or Co (Ⅲ), indicating that the Co element existence state was Co-N bond in Co-porous-g-C₃N₄. These results illustrate the Co-porous-g-C₃N₄ photocatalyst possesses great structural stability and the Co element was doped into g-C₃N₄ successfully.
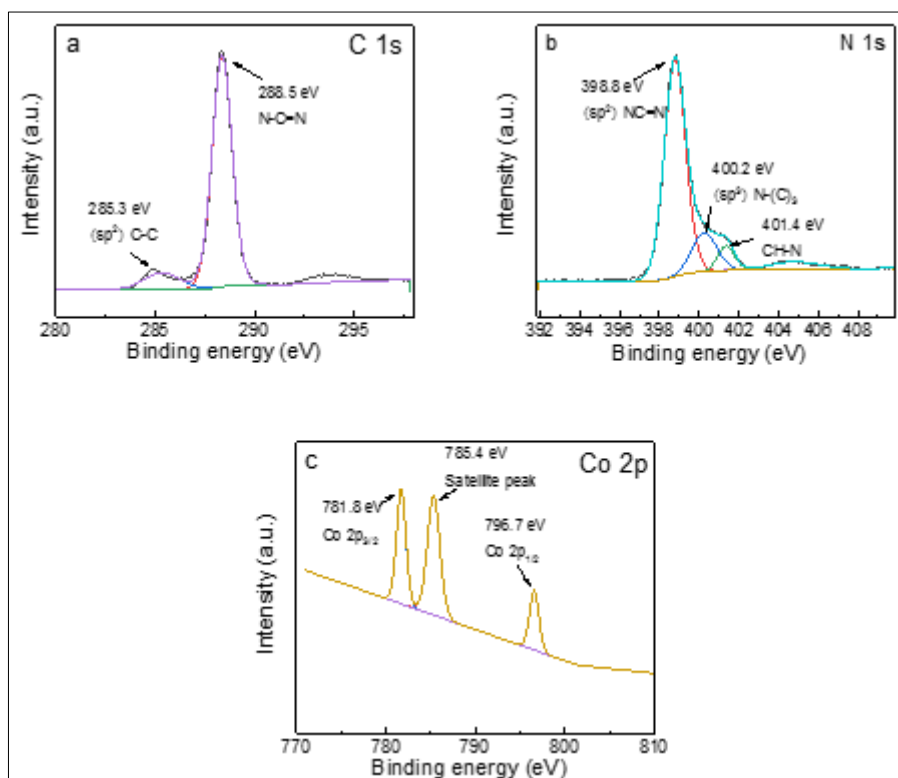


**Figure 3.** a) C 1s XPS spectra of Co-porous-g-C₃N₄, b) N 1s XPS spectra of Co-porous-g-C₃N₄, c) Co 2p XPS spectra of Co-porous-g-C₃N₄

The as-prepared Co-porous-g-C₃N₄ and g-C₃N₄ were further investigated by nitrogen adsorption and desorption isotherms (ASAP2460-2) in Figure 4. The isotherm of g-C₃N₄ shows a type IV [28], which

indicates the structure is mesopores (2 nm-50 nm) with a clear hysteretic regression line. However, the isotherm of Co-porous-g-$C_3N_4$ shows a type V due to the curve has not any inflection poins that is close to the x-axis in the low-medium pressure area and the force of between photocatalyst and nitrogen is weak. Besides, the type H3 hysteresis loop begins to appear in the medium pressure area, and the adsorption isotherm rises faster, which represents the adsorption isotherm feature of flake granular materials. These results indicate the Co-porous-g-$C_3N_4$ is mesoporous in a irregular structure and contain various forms of mesopores. Meanwhile, the surface area, pore size and volume of Co-porous-g-$C_3N_4$ photocatalyst are showed in Table 2, the surface area of Co-porous-g-$C_3N_4$ is 17.86 m$^2$/g, which is 3.74 times larger than g-$C_3N_4$ [28]. The average pore size of Co-porous-g-$C_3N_4$ is the almost same as g-$C_3N_4$, but the pore volume of Co-porous-g-$C_3N_4$ has about 5.5 times larger than g-$C_3N_4$.
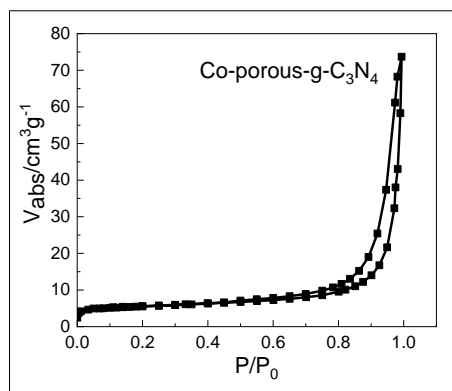


**Figure 4.** $N_2$-adsorption-desorption isotherm of Co-porous-g-$C_3N_4$

**Table 2.** BET specific surface area and pore size and volume of Co-porous-g-$C_3N_4$

| Sample | Surface area (m$^2$/g) | Pore size (nm) | Pore volume (cm$^3$/g) |
|---|---|---|---|
| Co-porous-g-$C_3N_4$ | 17.86 | 25.77 | 0.11 |

UV-Vis DRS spectra of Co-porous-g-$C_3N_4$ and g-$C_3N_4$ were performed in Figure 5. Unlike the typical light yellow of g-$C_3N_4$, the color of Co-porous-g-$C_3N_4$ is light green, the reason is that color is influenced by band gap. As shown in Figure 5, the absorption wavelength of 461 nm (g-$C_3N_4$) shift to 534 nm (Co-porous-g-$C_3N_4$) and the band gap can be calculated with $Eg = 1240/\lambda g$ (nm), the band gap of g-$C_3N_4$ (2.69 eV) changed to Co-porous-g-$C_3N_4$ (2.32 eV), with a decrease by 0.37 eV. The visible light responsiveness of Co-porous-g-$C_3N_4$ is enhanced with the decrease of the band gap, the utilization rate of visible light is increased. So the photocatalytic performance of Co-porous-g-$C_3N_4$ is improved.
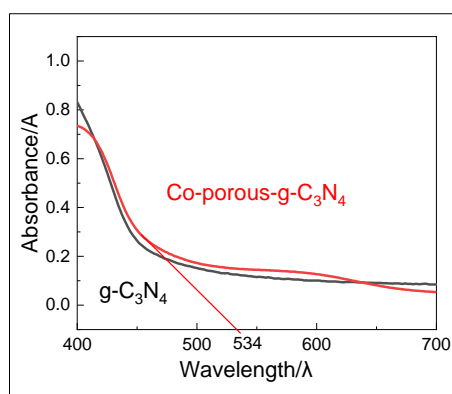


**Figure 5.** UV-DRS of Co-porous-g-$C_3N_4$

## 3.2. Photocatalytic degradation activity of Co-porous-g-C₃N₄ towards MB

For the sake of exploring the photocatalytic ability of Co-porous-g-C₃N₄, the degradation effect would be texted with MB model under a certain conditions and the consequences were showed in Figure 6. As depicted in Figure 6a, the doping amount of Co element was experimented, which the doping dosage was 0, 0.3, 0.6, 0.9, 1.2, 1.5 wt% under the treatment of 1 mL hydrochloric acid.
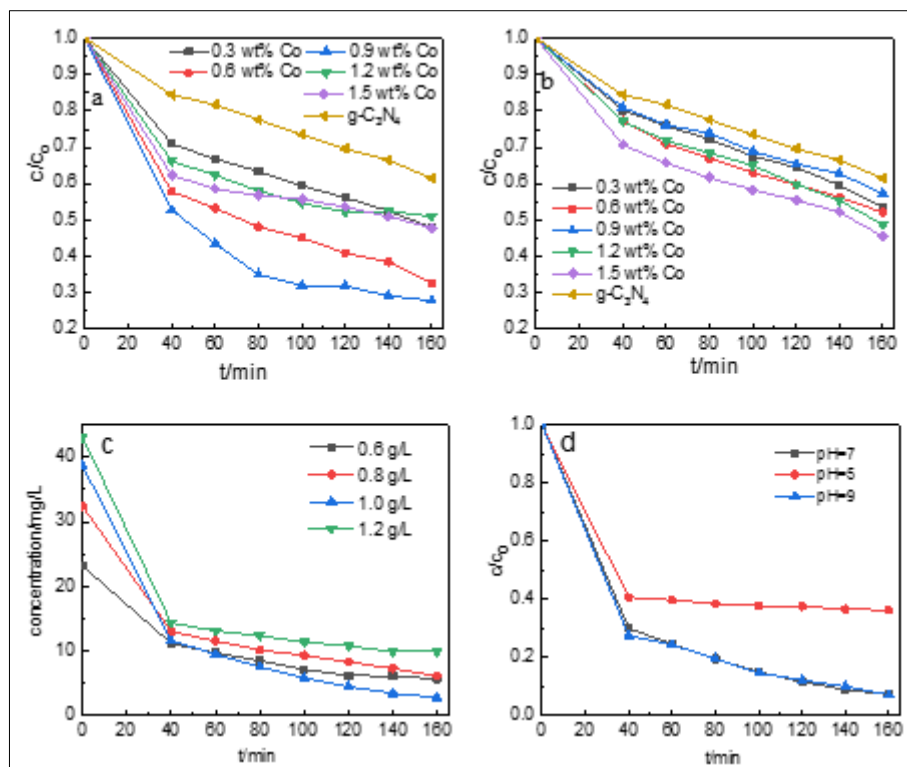


**Figure 6.** a) Effect of the doping amount of cobalt element-added hydrochloric acid,
b) Effect of the doping amount of cobalt element-no added hydrochloric acid
(MB = 10 mg/L, catalyst dose 0.6 g/L), c) Effect of the dose of Co-porous-g-C₃N₄ (MB = 23-43 mg/L), d) Effect of the *p*H (MB = 35 mg/L) , catalyst dose 1.0 g/L)

To explore the catalytic ability of Co-porous-g-C₃N₄ as a photocatalyst, the photocatalytic degradation of MB by Co-porous-g-C₃N₄ was investigated under certain conditions. As depicted in Figure 6a, the doping amount of Co element was experimented. The doping dosage was 0, 0.3, 0.6, 0.9, 1.2, 1.5 wt% under the treatment of 1 mL hydrochloric acid. When the doping dosage was 0.9 wt%, the degradation effect of MB was the best, and the degradation rate reached 72% at 120 min. It's worth noting that the photocatalytic effect would be decreased when the increasing of Co doping amount, and only half of MB could be degraded by that photocatalyst contained 1.2-1.5 wt% Co element. This may be due to the fact that the excessive doping of Co element will lead to the combination of catalyst active centers, which in turn affects the degradation performance of the catalyst. However, the photocatalyst without the treatment of 1 mL hydrochloric acid behaved worse in degrading MB under the same condition. When the doping dosage was 0.9 wt%, the degradation rate only reached 43% at 120 min in Figure 6b. But the degradation performance of the catalyst could also be improved due to the doping of Co.

In addition, the dose of Co-porous-g-C₃N₄ was explored from 0.6 g/L, 0.8 g/L, 1.0 g/L, to 1.2 g/L, and the results were showed in Figure 6c. In this reaction system, due to the different adsorption abilities of the different dose of Co-porous-g-C₃N₄, the concentration of MB had been controlled in 11-14 mg/L after 40 min adsorption in dark. And since there was some error in MB concentration (11-14 mg/L) at the end of the dark reaction, the degradation effect was compared by pure photocatalytic rate. The best

degradation was achieved when the dose of Co-porous-g-C$_3$N$_4$ was 1.0 g/L. The MB concentration decreased from 11.6 mg/L to 2.8 mg/L in 40-160 min, the pure photocatalytic degradation rate was 75.9%. When the doses of Co-porous-g-C$_3$N$_4$ were 0.6 g/L, 0.8 g/L and 1.2 g/L, the pure photocatalytic degradation rates were 49.1%, 52.3% and 31.3% respectively. Interestingly, when the dose was 1.2 g/L, the degradation effect decreased instead. The reason may be that excessive catalysts will accelerate the photogenerated electron-hole recombine rate and the simulated solar light source will be shaded. Therefore, the optimal dose of Co-porous-g-C$_3$N$_4$ was 1.0 g/L.

As showed in Figure 6d, the photocatalytic process was significantly inhibited which corresponding to a MB degradation rate of 64% when the MB solution was weakly acidic (*p*H=5). It could be attributed to the binding of H$^+$ in solution with photoelectrons, which inhibited the photocatalytic degradation process. However, the MB was basically completely degraded after 2 h, when the MB solution was neutral or weakly alkaline (*p*H=7, *p*H=9). It was more economical to choose neutral conditions (*p*H=7) as the optimal solution *p*H.
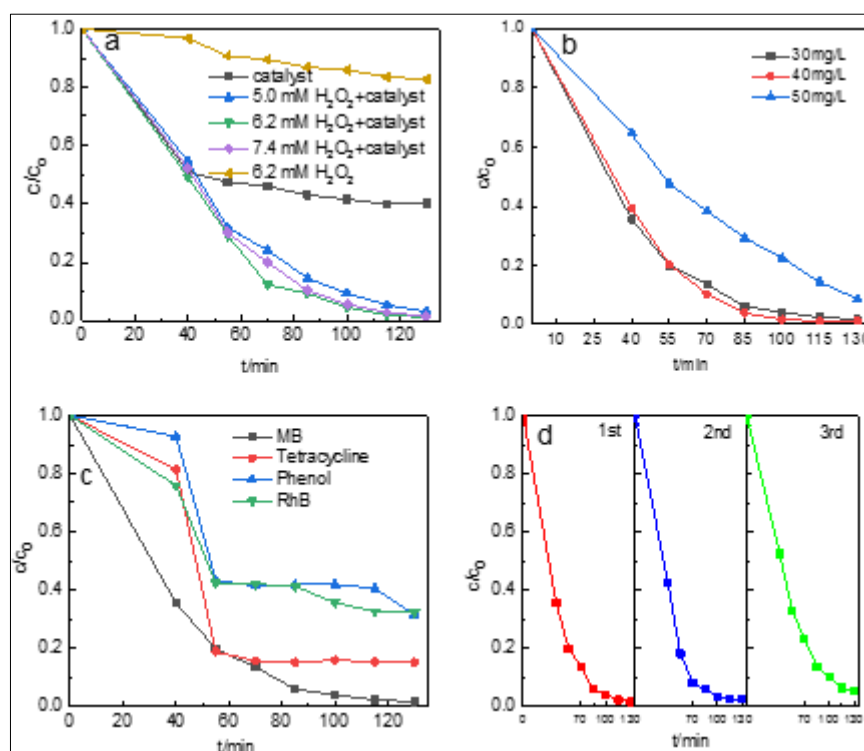


**Figure 7.** a) Effect of the dosage of H$_2$O$_2$ (MB=50 mg/L) b) Effect of the concentrations of MB (H$_2$O$_2$ =6.2 mmol/L) c) Degradation experiment of Co-porous-g-C$_3$N$_4$ on different organic pollutants (the concentration of neutral solution is 20 mg/L) d) Recyclability and stability of Co-porous-g-C$_3$N$_4$ (MB=30 mg/L)

As showed in Figure 7a, the degradation rates of MB were 60% and 18% at 90 min respectively when only Co-porous-g-C$_3$N$_4$ or H$_2$O$_2$ was applied. In contrast, the photocatalytic degradation performance could be enhanced substantially due to the construction of Photo-Fenton-like reaction system when Co-porous-g-C$_3$N$_4$ coexisted with H$_2$O$_2$. The degradation rate of MB could reach 95% when the dose of H$_2$O$_2$ (30%) was increased to 6.2 mmol/L. However, when the dose of H$_2$O$_2$ was increased to 7.2 mmol/L, the degradation rate of MB did not continue to increase but decreased. The reason may be that excess H$_2$O$_2$ can lead to low degradation rate due to the deactivation of active substances by violent collisions.

As shown in Figure 7b, Co-porous-g-C$_3$N$_4$ showed excellent photocatalytic effect when MB were 30 mg/L and 40 mg/L. The degradation rate could still reach 92% at 90 min when MB was increased to 50 mg/L. It can be seen that the high concentration MB could be degraded by Co-porous-g-C$_3$N$_4$ well.

Photocatalytic experiments were carried out with various organic pollutants, such as phenol, tetracycline and RhB (20mg/L). As showed in Figure 7c, different types of organic pollutants all could be degraded. The degradation effect of tetracycline was excellent. Thus, a variety of pollutants could be degraded by this system.

After completion of the single experiment, the catalyst was cleaned by physical methods such as simple ultrasonic treatment and rinsing. As showed in Figure 7d, the degradation rates of the three cycles were 99%, 98% and 95% respectively, indicating the wonderful stability of Co-porous-g-$C_3N_4$.
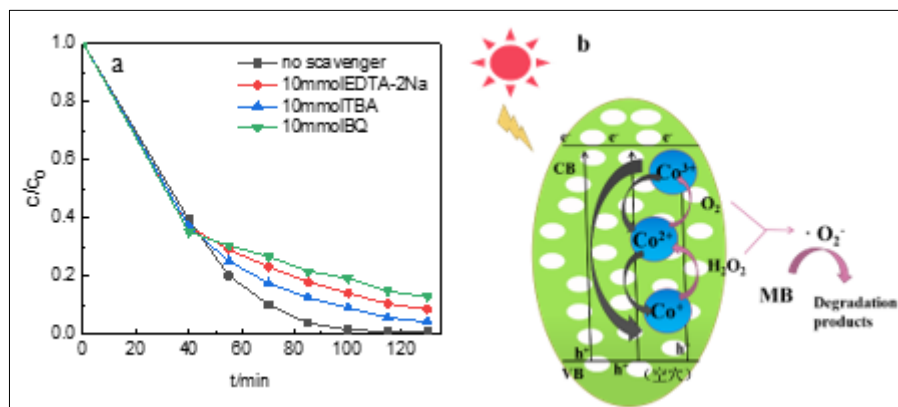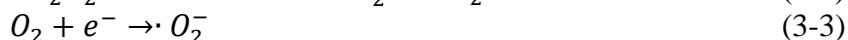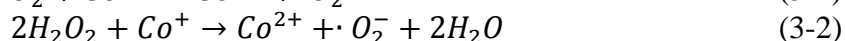


**Figure 8.** a) Free radical group of Co-porous-g-$C_3N_4$ (MB=40 mg/L)
b) The schematic diagram of the process

To explore the types of active species that play a major role in this system, radical quenching experiments were conducted. TBA, BQ and EDTA-2Na were used for quenching $\cdot$OH, $\cdot O_2$- and $h^+$, respectively. As shown in Figure 8a, the main degradation effect was attributed to $\cdot O_2$- while the secondary degradation effect was attributed to $h^+$ and $\cdot$OH. The mechanism of the degradation of organic pollutants by Co-porous-g-$C_3N_4$ was shown in Figure 8b.

Firstly, the holes with oxidation properties ($h^+$) could be formed by the photoelectron transitions. In addition, the reaction of $O_2$ with $Co^{2+}$ or $H_2O_2$ with $Co^+$ were both ways to generate $\cdot O_2$-(Eq. 3-1, Eq. 3-2 and Eq. 3-3). Finally, the circulation would be completed when High-valent cobalt turned to low-valent cobalt by absorbing photoelectrons (Eq. 3-4 and Eq. 3-5). The recombination rate of photogenerated electron-hole could be slowed down greatly in this system.

$$O_2 + Co^{2+} \rightarrow Co^{3+} + \cdot O_2^- \qquad (3\text{-}1)$$
$$2H_2O_2 + Co^+ \rightarrow Co^{2+} + \cdot O_2^- + 2H_2O \qquad (3\text{-}2)$$
$$O_2 + e^- \rightarrow \cdot O_2^- \qquad (3\text{-}3)$$
$$Co^{3+} + e^- \rightarrow Co^{2+} \qquad (3\text{-}4)$$
$$Co^{3+} + e^- \rightarrow Co^+ \qquad (3\text{-}5)$$

# 4. Conclusions

Highly active porous photocatalyst Co-porous-g-$C_3N_4$ was synthesized by calcination using cobalt chloride as source of Co and concentrated hydrochloric acid-treated melamine as precursor. Photo-Fenton-like reaction system was successfully constructed, and MB was almost completely degraded within 90 min with a degradation rate of 98.3%. Moreover, the catalytic degradation of various organic pollutants was also achieved. Through three recycling experiments, the good recyclability and stability of Co-porous-g-$C_3N_4$ were verified. And the main degradation effect was attributed to $\cdot O_2$-. In this study, the synergistic effect of Fenton-like system and photocatalysis was realized, which had a good application in degrading organic wastewater.

**Reference**

1.LIJUAN JIANG, YAJUN WANG, CHANGGEN FENG, 2012, Application of Photocatalytic Technology in Environmental Safety. Procedia Engineering 45: 993-997.

2.ABDURRAHMAN AKYOL, MAHMUT BAYRAMOGLU, 2007, The degradation of an azo dye in a batch slurry photocatalytic reactor. Chemical Engineering & Processing: Process Intensification 47: 2150-2156.

3.V. GOETZ, J.P., CAMBON, D., SACCO, G. PLANTARDET, 2008, Modeling aqueous hetero-geneous photocatalytic degradation of organic pollutants with immobilized $TiO_2$. Chemical Engineering & Processing: Process Intensification 48: 532-537.

4.LÍVIA N. RIBEIRO, ALINE C.S. FONSECA, EMERSON F.M. DA SILVA, EVELLE D.C. OLIVEIRA, ANDRÉ T.S. RIBEIRO, LAISSE C.A. MARANHÃO, JOSE G.A. PACHECO, GIOVANNA MACHADO, LUCIANO C. ALMEIDA, 2020, Residue-based $TiO_2$ /PET photocatalytic films for the degradation of textile dyes: A step in the development of green monolith reactors. Chemical Engineering and Processing - Process Intensification 147: 107792.

5.S SHUAISHUAI NI, YANJIE SU, ZHE AI, JING HU, ZHI YANG, ERIC SIU-WAI KONG, YAFEI ZHANG, 2016, Bandgap tuning and photocatalytic activities of CuSe1-xSx nanoflakes. Ceramics International 42: 211-219.

6.JUN ZHANG, PENGHUI TIAN, TAO TANG; GUOZHOU HUANG, JINGHUI ZENG, BO CUI, ZHENJIANG SHEN, HONGBO WANG, ZHE KONG, JUNHUA XI, ZHENGUO JI, (2020), Excellent photoelectrochemical hydrogen evolution performance of $FeSe_2$ nanorod/ZnSe 0D/1D heterostructure as efficiency carriers migrate channel. International Journal of Hydrogen Energy 45: 8526-8539.

7.HAIYAN LI, PUHUI DENG, YU HOU, 2018, Cobalt disulfide/graphitic carbon nitride as an efficient photocatalyst for hydrogen evolution reaction under visible light irradiation. Materials Letters 229: 217-220.

8.MARUTHATHURAI KASINATHAN, SIRVAKUMAR THIRIPURANTHAGAN, AISHWARYA SIVAKUMAR, 2020, A facile fabrication of Br-modified g-$C_3N_4$/rGO composite catalyst for enhanced visible photocatalytic activity towards the degradation of harmful dyes. Materials Research Bulletin 130: 110870.

9.GU ZHANYONG, ZHANG BIAO; ASAKURA YUSUKE, TSUKUDA SATOSHI, KATO HIDEKI, KAKIHANA MASATO, YIN SHU, 2020, Alkali-assisted hydrothermal preparation of g-$C_3N_4$/rGO nanocomposites with highly enhanced photocatalytic NOx removal activity. Applied Surface Science 521: 146213.

10.JIANQING MA, NANZHENGFANG JIA, CHENSI SHEN, WEIPING LIU, YUEZHONG WEN, 2019, Stable cuprous active sites in $Cu^+$-graphitic carbon nitride: Structure analysis and performance in Fenton-like reactions. Journal of Hazardous Materials 378: 120782.

11.G. MAMBA, A.K. MISHRA, 2016, Graphitic carbon nitride (g-$C_3N_4$) nanocomposites: A new and exciting generation of visible light driven photocatalysts for environmental pollution remediation. Applied Catalysis B: Environmental 198: 347-377.

12.YALIN YU, SHANGDI WU, JIAYU GU, RUI LIU, ZHE WANG, HUAN CHEN, FANG JIANG, 2020, Visible-light photocatalytic degradation of bisphenol A using cobalt-to-oxygen doped graphitic carbon nitride with nitrogen vacancies via metal-to-ligand charge transfer. Journal of Hazardous Materials 384: 121247.

13.YUNXIAO ZHANG, WEI-DE ZHANG, 2019, Ternary catalysts based on amino-functionalized carbon quantum dots, graphitic carbon nitride nanosheets and cobalt complex for efficient $H_2$ evolution under visible light irradiation. Carbon 145: 488-500.

14.NGUYEN DUC TRUNG, NGUYEN CHINH CHIEN, DO Trong on, 2020, Rational one-step synthesis of cobalt clusters embedded-graphitic carbon nitrides for the efficient photocatalytic CO2 reduction under ambient conditions. Journal of Catalysis 392: 88-96.

15.ZHONGCHUN LI, LEI WU, LIANGBIAO WANG, AIJUN GU, QUANFA ZHOU, 2017, Nickel cobalt sulfide nanosheets uniformly anchored on porous graphitic carbon nitride for supercapacitors with high cycling performance. Electrochimica Acta 231: 617-625.

16.KEYUN WANG, GUIZHOU GU, SHAOZHENG HU, JIAN ZHANG, XIAOLONG SUN, FEI WANG, PING LI, YANFENG ZHAO, ZHIPING FAN, XIONG ZOU, 2019, Molten salt assistant synthesis of three-dimensional cobalt doped graphitic carbon nitride for photocatalytic $N_2$ fixation: Experiment and DFT simulation analysis. Chemical Engineering Journal 368: 896-904.

17.SAMAHE SADJADI, MASOUMEH MALMIR, MAJID M. HERAVI, FATEMEH GHOREYSHI KAHANGI, 2019, Magnetic covalent hybrid of graphitic carbon nitride and graphene oxide as an efficient catalyst support for immobilization of Pd nanoparticles. Inorganica Chimica Acta 488: 62-70.

18.YUNJIN YAO, YI HU, HUANHUAN HU, LUWANG CHEN, MAOJING YU, MENGXUE GAO, SHAOBIN WANG, 2019, Metal-free catalysts of graphitic carbon nitride-covalent organic frameworks for efficient pollutant destruction in water. Journal of Colloid and Interface Science 554: 376-387.

19.FURONG GUO, JICHONG CHEN, JINGZHENG ZHAO, ZHUO CHEN, DONGSHENG XIA, ZHILAN ZHAN, QIANG WANG, 2021, Z-scheme heterojunction g-C3N4@PDA/BiOBr with biomimetic polydopamine as electron transfer mediators for enhanced visible-light driven degradation of sulfamethoxazole. Chemical Engineering Journal 386: 124014.

20.FEIFEI MEI, JINFENG ZHANG, CHANGHAO LIANG, KAI DAI, 2021, Fabrication of novel CoO/porous graphitic carbon nitride S-scheme heterojunction for efficient $CO_2$ photoreduction. Materials Letters 282: 128722.

21.MESGARI F, BEIGI SM, SALEHNIA F, HOSSEINI M, GANJALI MR, 2019, Enhanced electrochemi-luminescence of Ru(bpy)32+ by Sm2O3 nanoparticles decorated graphitic carbon nitride nano-sheets for pyridoxine analysis. Inorganic Chemistry Communications 106: 240-247.

22.YUAN A, LEI H, XI F, LIU J, QIN L, CHEN Z, DONG X, 2019, Graphene quantum dots decorated graphitic carbon nitride nanorods for photocatalytic removal of antibiotics. J Colloid Inter Sci 548: 56-65.

23.GUOHUI DONG, WINGKEI HO, YUHAN LI, LIZHI ZHANG, 2015, Facile synthesis of porous graphene-like carbon nitride ($C_6N_9H_3$) with excellent photocatalytic activity for NO removal. Applied Catalysis B: Environmental 174-175: 477-485.

24.***Wook Ahn, Moon Gyu Park, Dong Un Lee, Min Ho Seo, Gaopeng Jiang, Zachary P. Cano, Fathy Mohamed Hassan, Zhongwei Chen, 2018, Hollow Multivoid Nanocuboids Derived from Ternary Ni-Co-Fe Prussian Blue Analog for Dual-Electrocatalysis of Oxygen and Hydrogen Evolution Reactions. Advanced Functional Materials 28: 1802129.

25.AI JIANPING, ZHOU TAO, WANG XIPING, CHEN ZHIQIN, SHE YI, JIANG JIALI, CHEN JIANG, LI WENKUI, 2017, Synthesis and Characterization of Co-doped ZnO Powder and Its Photocatalytic Activity. Journal of Ceramics 38: 548-552.

26.YALIN YU, SHANGDI WU, JIAYU GU, RUI LIU, ZHE WANG, HUAN CHEN, FANG JIANG, 2020, Visible-light photocatalytic degradation of bisphenol A using cobalt-to oxygen doped graphitic carbon nitride with nitrogen vacancies via metal-to ligand charge transfer. Journal of Hazardous Materials 384: 121247.

27.D. DAS, D. BANERJEE, B. DAS, N.S. DAS, K.K. CHATTOPADHYAY, 2017, Effect of cobalt doping into graphitic carbon nitride on photo induced removal of dye from water. Materials Research Bulletin 89: 170-179.

28.BAI MAOJUAN, HUANG XUANYE, YIN HAN, NIU DELI, WAN JUN, 2021, Fe-Doped Graphitic Carbon Nitride for Methylene Blue Degradation with Visible-Light. Journal of nanoscience and nanotechnology 21: 5698-5706.